

Tissue attenuation imaging - Synthetic Aperture Focusing versus Spatial Compounding

Z. Klimonda, J. Litniewski, P. Karwat, W. Secomski, A. Nowicki,
Department of Ultrasound
Institute of Fundamental Technological Research
Warsaw, Poland
zklim@ipt.gov.pl

Abstract - The long term goal of this research is to develop the system enabling the imaging and quantitative measure of ultrasonic attenuation in tissue. It may support the diagnosis by accurate discrimination of the lesions from normal tissue at the early stage of the disease. The attenuation is estimated from the stochastic ultrasonic backscatter and time/spatial averaging is necessary to achieve reasonable accuracy. However the averaging worsens the spatial resolution. Two techniques of ultrasonic imaging, the Synthetic Aperture Focusing Technique (SAFT) and Spatial Compounding (SC), were applied and compared with respect to the quality of attenuation estimation. The ultrasonic RF data were collected from a tissue mimicking phantom using ultrasonic scanner (Ultrasonix SonixTOUCH). Both acquired echoes-sets were processed in the same way in order to calculate the downshift in a mean frequency f_m of the backscatter signal and resulting spatial distribution of attenuation coefficient. Compensation for the diffraction effects was included in the data processing. The RF data obtained with use of the SAFT proved to be more suitable for attenuation estimation.

I. INTRODUCTION

The images obtained with the standard ultrasonic scanners display the distribution of the tissue reflectivity that is related mostly to the tissue impedance variation. There are some other tissue parameters such as backscattering, attenuation and speed of sound that are strictly related to the tissue structure and could provide additional diagnostic value. It has been demonstrated that pathological tissue has different attenuation properties than the healthy one. In various publications it has been reported that pathological processes can lead to changes in the mean attenuation coefficient that range from several percent for cirrhotic human liver, through dozens percent for fatty human liver [5], or degenerated bovine articular cartilage [6] to over a hundred percent in case of porcine liver HIFU treatment *in vivo* [7] or two hundred percent for porcine kidney thermal coagulation [8]. These reports are a motivation for searching for the efficient methods of unambiguous attenuation estimation to be used in US imaging. The attenuation coefficient increases with frequency, thus it can be estimated from the variation of a

spectrum of backscattered echo signals. However, tests shows large variability of attenuation coefficient estimated through such method [9] introducing ambiguity and limiting the quality of tissue attenuation imaging. The variability of attenuation map can be reduced by means of averaging of several adjacent image lines at a cost of reduced lateral resolution. The effectiveness of averaging depends on the number of averaged lines and their statistical independence, which is inversely related to the acoustic beam width. The number of the image lines can be increased using the Spatial Compounding (SC) technique. The increase of statistical independence of the image lines can be obtained by means of Synthetic Aperture Focusing Technique (SAFT) – providing the dynamic focusing in the whole scanned area. Therefore, two above methods were used for acoustic data collecting that were subsequently processed for the attenuation estimation. The improvement of the quality of attenuation images for both SC and SAFT techniques was assessed in this approach.

II. METHODS

The ultrasonic wave propagating through the soft tissue is attenuated due to absorption and scattering. In soft tissue the attenuation coefficient depends on wave frequency and it is common to assume the linear relation between the attenuation and the frequency of the propagating ultrasonic wave [10]. The high frequency components of a propagating pulse spectrum are being attenuated stronger than low frequency components. This results in the virtual shift of pulse spectrum towards the lower frequencies. Assuming the Gaussian scanning pulses - and thus having the Gaussian shaped spectra - their mean frequency f_m can be expressed as follows [11]

$$f_m = f_0 - \frac{\alpha \cdot \Delta x \cdot \sigma^2}{2} \quad (1)$$

where f_0 is initial pulse mean frequency, σ^2 is the Gaussian variance of the pulse spectrum, Δx denotes penetrated distance and α is the attenuation coefficient. Gaussian pulse spectrum preserves the shape during propagation in linearly attenuating medium i.e. the σ^2 is constant. The attenuation coefficient can be calculated from the equation (1) as follows

$$\alpha = -\frac{2}{\sigma^2} \frac{\Delta f_m}{\Delta x} \xrightarrow{\Delta x \rightarrow 0} -\frac{2}{\sigma^2} \frac{df_m}{dx} \quad (2)$$

In our approach the mean frequency f_m is directly evaluated from the backscattered signal along the propagation path by means of the correlation estimator (IQ algorithm). The estimator is described by

$$f_m = \frac{1}{2\pi T_s} \operatorname{atan} \left(\frac{\sum_{i=1}^N Q(t(i))I(t(i)+T_s) - Q(t(i)+T_s)I(t(i))}{\sum_{i=1}^N I(t(i))I(t(i)+T_s) + Q(t(i)+T_s)Q(t(i))} \right) \quad (5)$$

where t is time, T_s is the sampling period and N is the estimator window length. The Q and I are quadrature and in-phase signal components and are obtained by quadrature sampling technique. The signal samples are numbered by index i . The quadrature sampling is often used in modern scanners and the correlation estimator is widely used in color Doppler mapping [12].

The resulting f_m line is next processed by Singular Spectrum Analysis (SSA) method [13] to obtain smooth, decreasing trend. The aim of the technique is the decomposition of the input data series into the sum of components which can be interpreted as the trend, oscillatory components and the noise (non-oscillatory components). The major applications of the SSA technique is the smoothing of the time series, finding the trend, forecasting and the detection of structural changes. There are two interesting features of the SSA in the context of the determining of the ultrasound attenuation profiles using signal's mean frequency changes. The first is that this is model-free technique – there is no need to know general function describing how the mean frequency changes with the depth. In fact, in the clinical situation there is no a priori knowledge about it. All we know is that the mean frequency changes comes from attenuation only, must be the strictly decreasing function of the path length, and that the local attenuation coefficient should be in some range which depends on the tissue type. The second feature of the SSA is the robustness to outliers. This is the important advantage as outliers could appear in the mean frequency from depth dependence of the real RF echoes from tissue. Moreover the SSA is easy to use – it need only one parameter – the window length.

The attenuation along the propagation path is calculated from this trend using eq.(2). In order to improve the uniformity of the attenuation images additional moving average filtration laterally, across several scanning lines, is performed. To diminish even farther the residual spatial variation of local attenuation data the additional processing – SAFT and SC – were used and compared.

In standard US the delay and sum based beamforming is used – its main limitation is that the quality of the images decreases as a distance from the beam focal point increases. This can be overcome by applying a multiple focus imaging, however it reduces a frame rate. There is no such disadvantage in SAFT providing good lateral resolution in the whole imaging area without reduction of the frame rate but for the price of additional data processing. In SAFT the single

or multiple set of elements from linear array is activated during transmission and reception allowing for dynamic focusing virtually at every image pixel. In our experiments we have used a single element transmission and full, 128 elements aperture reception (Fig. 1). The resulting SAFT reconstructed RF scan lines exhibit greater statistical independence than the ones recorded in standard beamforming. It allows to reduce the number of averaging when the attenuation is calculated.

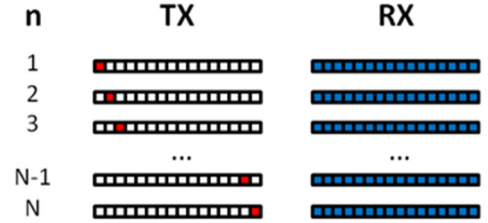


Fig. 1. The SAFT scheme using in this study. Single element transmit aperture and $N=128$ elements receiving aperture. The n represents successive transmissions.



Fig. 2. The idea of SC technique used in this study. The imaging plane changes through mechanically turning the probe.

The attenuation image quality can be also improved through a spatial compounding (SC) at the cost of decreasing frame-rate. This technique enables the probe to ‘look’ at the examined area at a number of angles (Fig. 2), what can be done electronically – by applying proper time delays, or mechanically – by tilting the probe. In this study the SC was performed mechanically. The final image is an average of images derived from several different, closely located scan planes. Such averaging significantly decrease the variation in the final attenuation map, comparing to the estimate variation in images derived from a single scan.

III. MEASUREMENTS

Experimental data were acquired from tissue mimicking phantom (1126-A, Dansk Phantom Service, Denmark) with uniform echogenicity and attenuation coefficient equal to

0.5 dB/cm/MHz. The phantom additionally contained a cylinder of 15mm in diameter located at 30mm depth. In terms of echogenicity the inclusion was indistinguishable from the surrounding medium. However, it had different attenuation coefficient value equal to 0.7 dB/cm/MHz. The data were collected using the SonixTOUCH scanner (Ultrasonix, Canada) with linear probe L14-5/38. The device allowed to record raw pre-beamformed data at sampling frequency of 40 MHz. Measurements were performed using two different transmit techniques: classical beamforming with spatial compounding and synthetic aperture focusing technique. The SC was done mechanically by tilting the probe in $\pm 10^\circ$ range around the array-phantom contact line. The resulting geometrical distortions were small in comparison to the resolving power of the attenuation imaging technique, thus were considered to be negligible. The focal point was located at 3cm depth. Short wide-band pulses of 8 MHz frequency were used as an excitation. The received RF echo signals were then reconstructed into RF image lines which were next analyzed for mean frequency changes as described in *Methods* section.

The second phantom (1126-B, Dansk Phantom Service, Denmark) with uniform attenuation of 0.5 dB/cm/MHz was used as a reference. The attenuation image of reference phantom for standard beamforming is shown in fig. 3. As it is shown the measured attenuation map is rather inhomogeneous, although the reference phantom has homogenous attenuation coefficient distribution. This effect is probably related to the spectral variations in the near field, focusing modifying pulse spectrum and influence of transducer transfer function. These overall changes of the pulse spectrum need to be compensated, to obtain proper attenuation estimate.

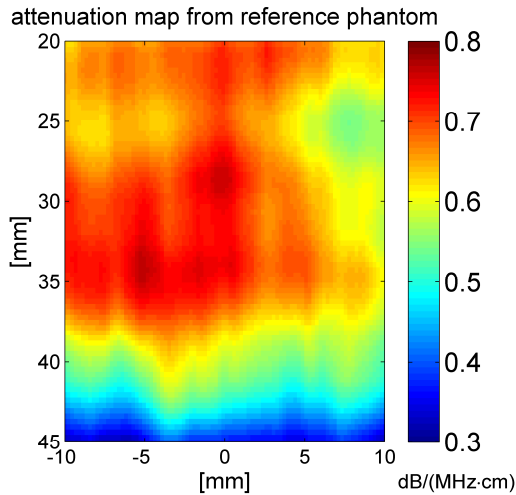


Fig. 4. The attenuation map of reference phantom obtained using standard beamforming.

Therefore the following procedure was applied: first, nine attenuation maps from reference phantom were estimated and next averaged for both beamforming and SAFT. In the next step the compensating factor was calculated as a ratio of the nominal attenuation (0.5 dB/cm/MHz) to the estimated

attenuation distribution of the reference phantom. Finally the compensating factor was used for the attenuation estimation in inhomogeneous phantom. The compensation of near field effects was realized by multiplication of the estimated attenuation map and the compensating factor.

IV. RESULTS

The B-mode image obtained using classical beamforming is presented in fig. 4. The cylindrical inclusion (marked with a white circle) is indistinguishable due to uniform echogenicity of the phantom. The presence of the attenuating object is manifested only by its acoustic shadow located beneath.

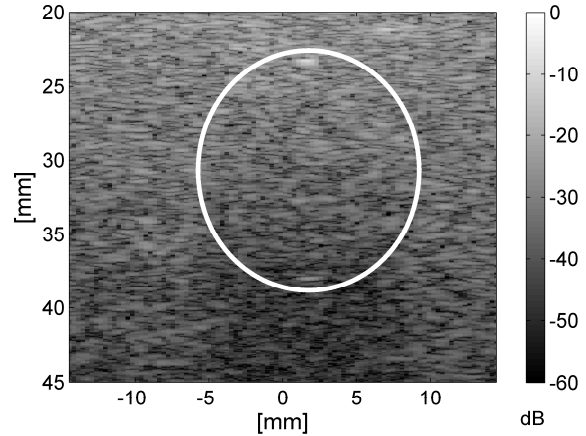


Fig. 4. The B-mode image of high attenuation area of the tissue phantom

In order to reveal the presence of the attenuation inhomogeneity, the attenuation imaging technique is applied. The single scan attenuation distribution image (Fig. 6) is of poor quality and the shape of the attenuating object is weakly mapped. The irregular, higher attenuating area is visible on the image, however the accuracy of the estimation based on standard beamforming is rather unacceptable. Therefore a modified data collection method was required.

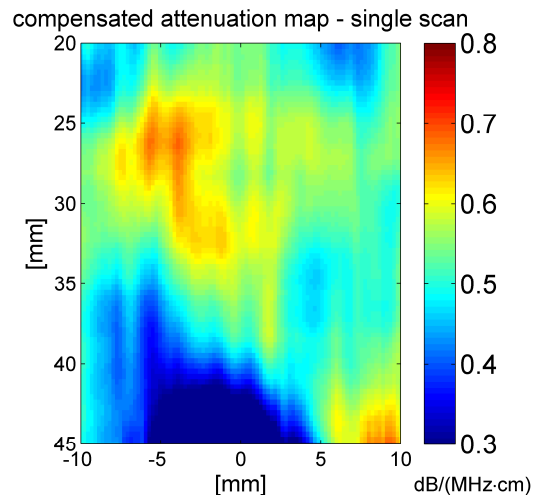


Fig. 6. The attenuation map of imaged object obtained using classical beamforming.

The attenuation maps obtained with use of the SC and SAFT are presented in figures 7 and 8, respectively. The highly attenuating area is clearly visible in both cases; however the SAFT image is by far of the better quality. In this case, the circular shape of the inclusion is clearly visible while in case of the SC image the shape is rather irregular. Moreover, there is an artifact visible at the SC image, beneath the attenuating region, which results from the weaker echo signal in acoustic shadow of the cylinder. There is no such artifact in SAFT image.

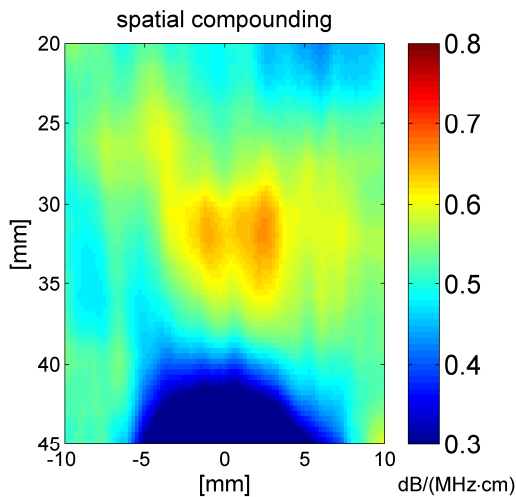


Fig. 7. The attenuation map of imaged object obtained using classical beamforming and SC technique

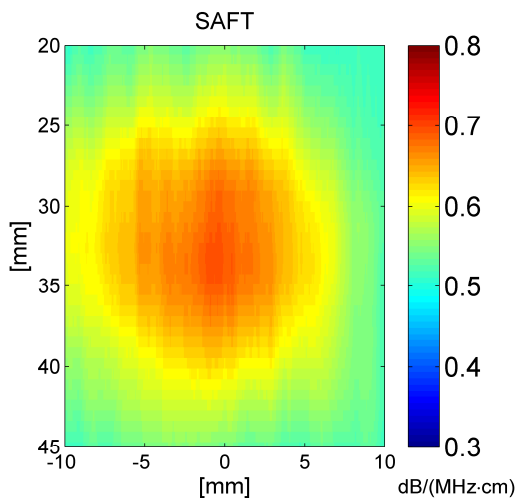


Fig. 8. The attenuation map of imaged object obtained using SAFT

V. CONCLUSIONS

The attenuation estimation method based on tracking of the spectral mean frequency shift is presented. The method was used to reconstruct the attenuation image of tissue phantom. In order to increase the quality of final images, the raw RF data were collected using two different methods – Spatial Compounding and Synthetic Aperture Focusing Technique. The attenuation imaging technique allowed to distinguish the object which was almost invisible in the classical B-mode

image. The object was detected by both SC and SAFT techniques, albeit the use of SAFT results in higher quality of the parametric image. The advantages of SAFT over the SC technique are better representation of the imaged object shape and lack of the shadow artifact. Furthermore, the SAFT technique requires single scan to produce a high quality attenuation map, thus it potentially allows to obtain higher frame rate at the cost of more complex numerical processing.

ACKNOWLEDGMENTS

This work has been in part supported with project 2011/01/B/ST7/06728 financed by polish National Science Centre and project POIG.01.03.01-14-012/08-00 co-financed by the European Regional Development Fund under the Innovative Economy Operational Programme. Project is governed by Ministry of Science and Higher Education, Poland.

REFERENCES

- [1] Oosterveld B. J., Thijssen J. M., Hartman P. C., Romijn R. L., Rosenbusch G. J.: Ultrasound attenuation and texture analysis of diffuse liver disease: methods and preliminary results. *Phys. Med. Biol.* Vol. 36 no. 8, 1991, pp. 1039–1064.
- [2] Saijo Y.: High Frequency Acoustic Properties of Tumor Tissue. In: *Ultrasonic Tissue Characterization*. Springer-Verlag Tokio (1996).
- [3] Bigelow, T. A., McFarlin, B. L., O'Brien, W. D., Oelze, M. L.: In vivo ultrasonic attenuation slope estimates for detection of cervical ripening in rats: Preliminary results, *Journal of Acoustical Society of America*, Vol. 123, No.3, 2008, pp. 1794-1800.
- [4] McFarlin B. L., Bigelow T. A., Laybed Y., O'Brien W. D., Oelze M. L., Abramowicz J. S.: Ultrasonic attenuation estimation of the pregnant cervix: a preliminary results, *Ultrasound in Obstetrics and Gynecology*, Vol. 36, 2010, pp. 218-225.
- [5] Lu Z., F., Zagzebski J., Lee F. T.: Ultrasound Backscatter and Attenuation in Human Liver With Diffuse Disease, *Ultrasound in Med. & Biol.* Vol. 25, No. 7, pp. 1047-1054, 1999.
- [6] Nieminen H. J., Saarakkala S., Laasanen M. S., Hirvonen J., Jurvelin J. S., Töyräs J.: Ultrasound Attenuation in Normal and Spontaneously Degenerated Articular Cartilage, *Ultrasound in Med. & Biol.* Vol. 30, No. 4, 2004, pp. 493-500.
- [7] Zderic V., Keshavarzi A., Andrew A. M., Vaezy S., Martin R. W. Attenuation of Porcine Tissues In Vivo After High Intensity Ultrasound Treatment, *Ultrasound in Med. & Biol.* Vol. 30, No. 1, 2004, pp. 61-66.
- [8] Worthington A., E., Sherar M., D., Changes in Ultrasound Properties of Porcine Kidney Tissue During Heating, *Ultrasound in Med. & Biol.* Vol. 27, No. 5, 2001, pp. 673-682.
- [9] Klimonda, Z., Litniewski, J., Nowicki, A.: Spatial Resolution of Attenuation Imaging, *Archives of Acoustics*, Vol. 34, No. 4, 2009, pp. 461-470.
- [10] Cobbold R. S. C., *Foundations of Biomedical Ultrasound*, Oxford University Press, 2007.
- [11] Laugier P., Berger G., Fink M., Perrin J.: Specular reflector noise: effect and correction for in vivo attenuation estimation. *Ultras. Imag.* Vol. 7, 1985, 277-292.
- [11] Evans D. H., McDicken W. N.: *Doppler Ultrasound: Physics, Instrumentation and Signal Processing*, John Wiley & Sons Ltd., 2000.
- [13] Golyandina, N., Nekrutkin, V., Ahigljavsky, A.: *Analysis of time Series Structure: SSA and related techniques*, Chapman & Hall/CRC, 2001.